C^1 Hermite interpolation with spatial Pythagorean-hodograph cubic biarcs

Bohumír Bastl[a], Michal Bizzarri[b,a], Marjeta Krajnc[d], Miroslav Lávička[a,b], Kristýna Slabá[a], Zbyněk Šír[c], Vito Vitrih[e], Emil Žagar[d,*]

[a]*University of West Bohemia, Faculty of Applied Sciences, Department of Mathematics, Univerzitní 8, 301 00 Plzeň, Czech Republic*
[b]*NTIS – New Technologies for Information Society, Faculty of Applied Sciences, University of West Bohemia, Univerzitní 8, 301 00 Plzeň, Czech Republic*
[c]*Charles University in Prague, Faculty of Mathematics and Physics, Sokolovská 83, 186 75 Prague, Czech Republic*
[d]*University of Ljubljana, IMFM and FMF, Jadranska 19, Ljubljana, Slovenia*
[e]*University of Primorska, IAM and FAMNIT, Muzejski trg 2, Koper, Slovenia*

Abstract

In this paper the C^1 Hermite interpolation problem by spatial Pythagorean-hodograph cubic biarcs is presented and a general algorithm to construct such interpolants is described. Each PH cubic segment interpolates C^1 data at one point and they are then joined together with a C^1 continuity at some unknown common point sharing some unknown tangent vector. Biarcs are expressed in a closed form with three shape parameters. Two of them are selected based on asymptotic approximation order, while the remaining one can be computed by minimizing the length of the biarc or by minimizing the elastic blending energy. The final interpolating spline curve is globally C^1 continuous, it can be constructed locally and it exists for arbitrary Hermite data configurations.

Keywords:
Pythagorean-hodograph, Hermite, interpolation, biarc, cubic, spatial

1. Introduction

Pythagorean-hodograph (or shortly PH) curves form a special subclass of parametric curves which have several important properties, such as a (piecewise) polynomial arc length and a rational offset. This makes them very useful in many practical applications, such as CAGD, CAD/CAM systems, CNC machining, robotics, animation ... They were first introduced in [1] and since then, many approximation and interpolation schemes that involve PH curves can be found in the literature. Interpolation methods by general polynomial curves are usually based on low degrees polynomials, i.e., up to 5. Since only odd degree PH curves are regular, this practically reduces interpolation methods by such curves to cubic and quintic cases.

For planar cubic PH curves one of the first interpolation methods was given in [2] where G^1 interpolation of Hermite data (i.e. positions and tangent directions) at two given points was analyzed, and in [3], where G^1 and C^1 Hermite interpolation via double-Tschirnhausen cubics have been considered. These results were later generalized in [4] to G^2 interpolation by the same objects, and in [5], where a thorough analysis of the number of solutions and their properties was done. For quintic planar PH curves, several results on first and second order continuous spline interpolation are given in [6], [7], [8], [9], [10], [11] ... For spatial curves, G^1 Hermite interpolation by PH cubics was thoroughly investigated in [12]. Those results were later generalized to some level in [13]. The most general results on this type of interpolation can be found in [14] and [15]. The problem of C^1 and C^2 Hermite interpolation by spatial PH curves of degree ≥ 5 has been studied in [16], [17], [18], [19] ...

*Corresponding author
Email addresses: bastl@kma.zcu.cz (Bohumír Bastl), bizzarri@kma.zcu.cz (Michal Bizzarri), marjetka.krajnc@fmf.uni-lj.si (Marjeta Krajnc), lavicka@kma.zcu.cz (Miroslav Lávička), kslaba@kma.zcu.cz (Kristýna Slabá), zbynek.sir@gmail.com (Zbyněk Šír), vito.vitrih@upr.si (Vito Vitrih), emil.zagar@fmf.uni-lj.si (Emil Žagar)

Since C^1 Hermite interpolation by cubic polynomial spline curves is always uniquely solvable, it is clear that the same problem can not be solved by PH cubic splines. However, low degree polynomial interpolating splines are important in several applications, and one would insist on using cubic curves. One possibility is to relax C^1 continuity to G^1 continuity but unfortunately it is not always possible to interpolate G^1 Hermite data by PH cubic (see [12], [14] and [15], e.g.). To avoid this, C^1 Hermite iterpolation by spatial PH biarcs will be considered in this paper. This approach is a generalization of C^1 Hermite interpolation with planar uniform and non-uniform cubic PH biarcs which was recently studied in [20]. The idea is to join two arcs of spatial cubic PH curves at some unknown point. First curve interpolates C^1 Hermite data at one side, and the other one interpolates the same type of data at the other side. The arcs are then joined together with C^1 continuity in order to make the final biarc C^1 smooth. It turns out that the biarc depends on three shape parameters. The final interpolating spline curve is globally C^1 continuous, it can be constructed locally and it exists for arbitrary Hermite data configurations.

The paper is organized as follows. In Section 2 the theory of quaternions and the connection between quaternions and spatial PH curves is briefly recalled. Next section describes the Hermite C^1 interpolation problem by spatial cubic PH biarcs and presents a general algorithm for computing interpolants. In Section 4 the asymptotic behaviour of solutions with respect to two shape parameters is studied and in the following section the parameter values which preserve planarity are identified. In the last section the computation of the last shape parameter is considered and several criteria how to choose it are provided. The paper is concluded with Section 7 that summarizes the main results of the paper and identifies possible future investigations.

2. Quaternions and spatial PH curves

As the planar PH curves can be defined through some relations between complex numbers (see, e.g., [21]), the spatial PH curves can be determined by relations between quaternions or through a Hopf map representation ([11]). Quaternions form a 4-dimensional vector space $\mathbb{H}$ with a standard basis $\{\mathbf{1}, \mathbf{i}, \mathbf{j}, \mathbf{k}\}$,

$$\mathbf{1} = (1,0,0,0), \quad \mathbf{i} = (0,1,0,0), \quad \mathbf{j} = (0,0,1,0), \quad \mathbf{k} = (0,0,0,1).$$

The first component of a quaternion is called a scalar part, while the remaining three components form a vector part of a quaternion. A quaternion with a zero scalar part is called a pure quaternion. Vectors in $\mathbb{R}^3$ can be identified with pure quaternions and vice versa. For quaternions $\mathcal{A} = (a, \boldsymbol{a})$ and $\mathcal{B} = (b, \boldsymbol{b})$, $a, b \in \mathbb{R}$, $\boldsymbol{a}, \boldsymbol{b} \in \mathbb{R}^3$, we can define

$$\mathcal{A} + \mathcal{B} = (a + b, \boldsymbol{a} + \boldsymbol{b}), \quad \mathcal{A}\mathcal{B} = (ab - \boldsymbol{a} \cdot \boldsymbol{b}, a\boldsymbol{b} + b\boldsymbol{a} + \boldsymbol{a} \times \boldsymbol{b}).$$

With this associative, but noncommutative multiplication the space of quaternions becomes an algebra. Moreover, $\bar{\mathcal{A}} := (a, -\boldsymbol{a})$ denotes a conjugate of $\mathcal{A}$ and the norm of a quaternion $\mathcal{A}$ is defined as

$$\|\mathcal{A}\|^2 = \bar{\mathcal{A}}\mathcal{A} = \mathcal{A}\bar{\mathcal{A}} = a^2 + \|\boldsymbol{a}\|^2,$$

where $\|\boldsymbol{a}\| = \sqrt{\boldsymbol{a} \cdot \boldsymbol{a}}$ is the Euclidean norm of the vector $\boldsymbol{a}$. We can also define a commutative multiplication on the space of quaternions as

$$\mathcal{A} \star \mathcal{B} := \frac{1}{2}(\mathcal{A}\,\mathbf{i}\,\bar{\mathcal{B}} + \mathcal{B}\,\mathbf{i}\,\bar{\mathcal{A}}). \tag{1}$$

By this operation $\mathcal{A} \star \mathcal{B}$ is a pure quaternion and will be identified with a vector in $\mathbb{R}^3$ several times later on. In order to simplify the notation, the expression $\mathcal{A}^{2\star} := \mathcal{A} \star \mathcal{A}$ will be used.

By [22] it is easy to solve a 'quadratic' $\star$–equation which is recalled in the following lemma.

Lemma 1. *Let $\mathcal{A}$ be a given pure quaternion. All the solutions of a quadratic $\star$–equation $\mathcal{X}^{2\star} = \mathcal{A}$ form a one–parameter family*

$$\mathcal{X} := \mathcal{X}(\varphi; \mathcal{A}) := \mathcal{X}_p(\mathcal{A})\mathcal{Q}_\varphi, \quad \mathcal{Q}_\varphi := \cos\varphi + \mathbf{i}\,\sin\varphi, \;\; \varphi \in [-\pi, \pi), \tag{2}$$

where $\mathcal{X}_p(\mathcal{A})$ is a particular solution given by

$$\mathcal{X}_p(\mathcal{A}) := \begin{cases} \sqrt{\|\mathcal{A}\|}\,\dfrac{\frac{\mathcal{A}}{\|\mathcal{A}\|}+\mathbf{i}}{\left\|\frac{\mathcal{A}}{\|\mathcal{A}\|}+\mathbf{i}\right\|} & \frac{\mathcal{A}}{\|\mathcal{A}\|} \neq -\mathbf{i} \\ \sqrt{\|\mathcal{A}\|}\,\mathrm{k} & \frac{\mathcal{A}}{\|\mathcal{A}\|} = -\mathbf{i} \end{cases}.$$

Moreover, it is not difficult to see that for any quaternions $\mathcal{A}$ and $\mathcal{B}$

$$\mathcal{A}\mathcal{Q}_\varphi \star \mathcal{B}\mathcal{Q}_\psi = \mathcal{A}\mathcal{Q}_{\varphi-\psi} \star \mathcal{B} = \mathcal{A} \star \mathcal{B}\mathcal{Q}_{\psi-\varphi}. \tag{3}$$

Let us now define the connection between spatial PH curves and quaternions (see, e.g., [11]). The hodograph of a spatial polynomial curve $\boldsymbol{p}(t) = (x(t), y(t), z(t))^\top$ of degree n is the curve $\boldsymbol{h}(t) := \boldsymbol{p}'(t) = (x'(t), y'(t), z'(t))^\top$ of degree $n-1$, where $\boldsymbol{p}'$ denotes the derivative of $\boldsymbol{p}$ with respect to the parameter t. Such a polynomial curve is called Pythagorean-Hodograph curve (PH curve), if the Euclidean norm of its hodograph is a piecewise polynomial function of degree $n-1$. More precisely, there must exist a polynomial σ, such that

$$x'(t)^2 + y'(t)^2 + z'(t)^2 = \sigma^2(t).$$

If all real roots of $\gcd(x', y', z')$ have even multiplicity, then $\boldsymbol{p}$ is a PH curve iff there exist polynomials u, v, p, q such that

$$x' = u^2 + v^2 - p^2 - q^2, \quad y' = 2uq + 2vp, \quad z' = 2vq - 2up, \quad \sigma = u^2 + v^2 + p^2 + q^2.$$

This gives use the following lemma.

Lemma 2. *Let $\boldsymbol{p}(t) = x(t)\mathbf{i} + y(t)\mathbf{j} + z(t)\mathbf{k}$ be a spatial polynomial curve, such that all real roots of $\gcd(x', y', z')$ have even multiplicity. Then $\boldsymbol{p}$ is a PH curve iff there exists a quaternion polynomial $\mathcal{A}(t) = u(t) + v(t)\mathbf{i} + p(t)\mathbf{j} + q(t)\mathbf{k}$, such that*

$$\boldsymbol{h}(t) = \mathcal{A}(t)\mathbf{i}\bar{\mathcal{A}}(t) = \mathcal{A}(t)^{2\star}.$$

The quaternion curve $\mathcal{A}(t)$ is called the preimage. Note that quaternions $\mathcal{A}(t)$ and $\mathcal{A}(t)\mathcal{Q}_\phi$ generate the same hodograph.

3. Interpolation problem and algorithm

In this section the interpolation problem by spatial cubic PH biarcs is presented and an algorithm for computing interpolants is given. Let $\boldsymbol{P}_0, \boldsymbol{P}_2 \in \mathbb{R}^3$ be two given points and let $\boldsymbol{t}_0$ and $\boldsymbol{t}_2$ be given associated tangent vectors. Our goal is to find a *PH cubic biarc* interpolant $\boldsymbol{p}_\tau : [0,1] \to \mathbb{R}^3$, composed of two spatial cubic PH curves $\boldsymbol{b} : [0,\tau] \to \mathbb{R}^3$ and $\boldsymbol{c} : [\tau,1] \to \mathbb{R}^3$, $\tau \in (0,1)$, i.e.,

$$\boldsymbol{p}_\tau(t) = \begin{cases} \boldsymbol{b}(t), & t \in [0,\tau], \\ \boldsymbol{c}(t), & t \in [\tau,1], \end{cases} \tag{4}$$

such that

$$\boldsymbol{b}(0) = \boldsymbol{P}_0, \quad \boldsymbol{b}'(0) = \boldsymbol{t}_0, \quad \boldsymbol{c}(1) = \boldsymbol{P}_2, \quad \boldsymbol{c}'(1) = \boldsymbol{t}_2. \tag{5}$$

Additionally we require that curves $\boldsymbol{b}$ and $\boldsymbol{c}$ join with the C^1 continuity at some unknown common point sharing some unknown tangent vector,

$$\boldsymbol{P}_1 := \boldsymbol{b}(\tau) = \boldsymbol{c}(\tau), \quad \boldsymbol{t}_1 := \boldsymbol{b}'(\tau) = \boldsymbol{c}'(\tau). \tag{6}$$

In order to use Bézier representation of spatial cubic PH curves it is appropriate to express $\boldsymbol{b}$ and $\boldsymbol{c}$ in a Bézier form as

$$\boldsymbol{b}(t) = \sum_{j=0}^{3} \boldsymbol{b}_j\, B_j^3\left(\frac{t}{\tau}\right), \quad t \in [0,\tau], \qquad \boldsymbol{c}(t) = \sum_{j=0}^{3} \boldsymbol{c}_j\, B_j^3\left(\frac{t-\tau}{1-\tau}\right), \quad t \in [\tau,1], \tag{7}$$

where $\boldsymbol{b}_j$ and $\boldsymbol{c}_j$, $j = 0, 1, 2, 3$, are control points and

$$B_j^n(t) = \binom{n}{j} t^j (1-t)^{n-j}, \quad j = 0, 1, \ldots, n,$$

are the Bernstein basis polynomials.

By using the quaternion representation of spatial PH cubics [11], the preimages of both arcs can be described as

$$\mathcal{B}(u) = \mathcal{B}_0(1-u) + \mathcal{B}_1 u, \qquad \mathcal{C}(u) = \mathcal{C}_0(1-u) + \mathcal{C}_1 u, \quad u \in [0,1], \tag{8}$$

where $\mathcal{B}_i, \mathcal{C}_i \in \mathbb{H}$, $i = 1, 2$, and for the control points of the curves $\boldsymbol{b}$ and $\boldsymbol{c}$ it holds

$$\begin{aligned} \boldsymbol{b}_1 &= \boldsymbol{b}_0 + \tfrac{1}{3}\mathcal{B}_0^{2\star}, & \boldsymbol{c}_1 &= \boldsymbol{c}_0 + \tfrac{1}{3}\mathcal{C}_0^{2\star}, \\ \boldsymbol{b}_2 &= \boldsymbol{b}_1 + \tfrac{1}{3}\mathcal{B}_0 \star \mathcal{B}_1, & \boldsymbol{c}_2 &= \boldsymbol{c}_1 + \tfrac{1}{3}\mathcal{C}_0 \star \mathcal{C}_1, \\ \boldsymbol{b}_3 &= \boldsymbol{b}_2 + \tfrac{1}{3}\mathcal{B}_1^{2\star}, & \boldsymbol{c}_3 &= \boldsymbol{c}_2 + \tfrac{1}{3}\mathcal{C}_1^{2\star}. \end{aligned} \tag{9}$$

Standard properties of Bézier curves (see, e.g, [23]), equations (9) and the interpolation conditions (5) imply

$$\boldsymbol{b}_0 = \boldsymbol{P}_0, \quad \mathcal{B}_0^{2\star} = \tau\, \boldsymbol{t}_0, \quad \boldsymbol{c}_3 = \boldsymbol{P}_2, \quad \mathcal{C}_1^{2\star} = (1-\tau)\, \boldsymbol{t}_2. \tag{10}$$

Moreover, C^1 condition (6) implies

$$\mathcal{C}_0^{2\star} = \frac{1-\tau}{\tau}\, \mathcal{B}_1^{2\star}. \tag{11}$$

By (2), (10) and (11) it follows

$$\begin{aligned} &\mathcal{B}_0 = \mathcal{X}(\varphi_0; \tau \boldsymbol{t}_0), \\ &\mathcal{C}_1 = \mathcal{X}(\psi_1; (1-\tau)\boldsymbol{t}_2), \\ &\mathcal{C}_0 = \sqrt{\frac{1-\tau}{\tau}}\, \mathcal{B}_1 \mathcal{Q}_{\psi_0}. \end{aligned} \tag{12}$$

It is straightforward to see from (3) and (9) that the same control points $\boldsymbol{c}_i$, $i = 0, 1, 2, 3$, are obtained if we choose

$$\mathcal{C}_0 = \sqrt{\frac{1-\tau}{\tau}}\, \mathcal{B}_1 \quad \text{and} \quad \mathcal{C}_1 = \mathcal{X}(\psi_1 - \psi_0; (1-\tau)\boldsymbol{t}_2).$$

Finally, (6) and (9) imply the following quaternion quadratic equation for $\mathcal{B}_1$

$$\mathcal{B}_1^{2\star} + \mathcal{B}_1 \star \mathcal{D} + \mathcal{E} = 0, \tag{13}$$

where

$$\begin{aligned} &\mathcal{D} := \tau\, \mathcal{X}(\varphi_0; \tau \boldsymbol{t}_0) + \sqrt{\tau(1-\tau)}\, \mathcal{X}(\psi_1 - \psi_0; (1-\tau)\boldsymbol{t}_2), \\ &\mathcal{E} := 3\tau(\boldsymbol{P}_0 - \boldsymbol{P}_2) + \tau^2\, \boldsymbol{t}_0 + \tau(1-\tau)\boldsymbol{t}_2. \end{aligned} \tag{14}$$

By transforming the equation (13) into

$$\left(\mathcal{B}_1 + \frac{1}{2}\mathcal{D}\right)^{2\star} = \frac{1}{4}\mathcal{D}^{2\star} - \mathcal{E},$$

we obtain a one-parameter family of solutions for the unknown quaternion $\mathcal{B}_1$, namely

$$\mathcal{B}_1 = -\frac{1}{2}\mathcal{D} + \mathcal{X}\left(\varphi_1; \frac{1}{4}\mathcal{D}^{2\star} - \mathcal{E}\right) = \left(-\frac{1}{2}\mathcal{F} + \mathcal{X}_p\left(\frac{1}{4}\mathcal{F}^{2\star} - \mathcal{E}\right)\right)\mathcal{Q}_{\varphi_1}, \quad \mathcal{F} := \mathcal{D}\mathcal{Q}_{-\varphi_1}. \tag{15}$$

From (1), (3), (9), (12), (13) and (15) now follows that control points $\boldsymbol{b}_i$ and $\boldsymbol{c}_i$, $i = 0, 1, 2, 3$, do not change if we take

$$\begin{aligned} &\mathcal{B}_0 := \mathcal{B}_0(\alpha) = \mathcal{X}(\alpha; \tau \boldsymbol{t}_0), \quad \mathcal{C}_1 := \mathcal{C}_1(\beta) = \mathcal{X}(\beta; (1-\tau)\boldsymbol{t}_2), \\ &\mathcal{B}_1 := \mathcal{B}_1(\alpha, \beta) = -\frac{1}{2}\mathcal{F} + \mathcal{X}_p\left(\frac{1}{4}\mathcal{F}^{2\star} - \mathcal{E}\right), \quad \mathcal{C}_0 := \mathcal{C}_0(\alpha, \beta) = \sqrt{\frac{1-\tau}{\tau}}\mathcal{B}_1, \end{aligned} \tag{16}$$

where

$$\alpha := \varphi_0 - \varphi_1, \quad \beta := \psi_1 - \psi_0 - \varphi_1, \quad \mathcal{F} = \mathcal{F}(\alpha, \beta) = \tau\mathcal{B}_0 + \sqrt{\tau(1-\tau)}\mathcal{C}_1$$

and $\mathcal{E}$ is given in (14). Let us summarize the results in the following theorem:

Theorem 1. *Let $\boldsymbol{P}_i, \boldsymbol{t}_i$, $i = 0, 2$, be given non-degenerate spatial Hermite data and let $\tau \in (0, 1)$. Then there exists a two-parameter family of interpolating PH cubic biarcs $\boldsymbol{p}_\tau(t; \alpha, \beta)$, given by* (4)*,* (7)*,* (8)*,* (9) *and* (16)*, satisfying* (5) *and* (6)*.*

Let $\boldsymbol{P}_i, \boldsymbol{t}_i$, $i = 0, 2$, be given data and let $\boldsymbol{p}_\tau(t; \alpha, \beta) : [0, 1] \to \mathbb{R}^3$ be an interpolating PH cubic biarc with respect to chosen parameters α and β. Further, let Φ be an orthogonal transformation and $\widetilde{\boldsymbol{p}}_\tau(t; \alpha, \beta) : [0, 1] \to \mathbb{R}^3$ be an interpolant with respect to the transformed data $\widetilde{\boldsymbol{P}}_0$, $\widetilde{\boldsymbol{P}}_2$, $\widetilde{\boldsymbol{t}}_0$, $\widetilde{\boldsymbol{t}}_2$. In general

$$\Phi\left(\boldsymbol{p}_\tau(t; \alpha, \beta)\right) = \widetilde{\boldsymbol{p}}_\tau(t; \widetilde{\alpha}, \widetilde{\beta}) \quad \Rightarrow \quad (\alpha, \beta) \neq (\widetilde{\alpha}, \widetilde{\beta}), \tag{17}$$

except for some particular cases (see [16]). Note that a general relation between (α, β) and $(\tilde{\alpha}, \tilde{\beta})$ such that the left-hand side of (17) would hold, is quite complicated.

As one can expect from the planar case ([20]), not all choices of parameters α and β will provide the same approximation order of corresponding interpolants. In order to determine which solutions are more acceptable from the approximation point of view, it is by (17) very important to choose a particular position of data, to which the original data should be transformed before the asymptotic analysis is done. Since by [16, Lemma 3] the following properties hold:

- if Φ is a rotation about the **i**-axis, then $\widetilde{\boldsymbol{p}}_\tau(t; \alpha, \beta) = \Phi\left(\boldsymbol{p}_\tau(t; \alpha, \beta)\right)$,
- if Φ is a reflection with respect to a plane containing the **i**-axis, then $\widetilde{\boldsymbol{p}}_\tau(t; \alpha, \beta) = \Phi\left(\boldsymbol{p}_\tau(t; -\alpha, -\beta)\right)$,

good choices are the following so-called *standard positions* of the data.

Definition 1. *The C^1 spatial Hermite data $\boldsymbol{P}_i$, $\boldsymbol{t}_i$, $i = 0, 2$, are said to be in a standard position, if $\boldsymbol{t}_0 + \boldsymbol{t}_2$ is a positive multiple of* **i***, and $\boldsymbol{P}_0 = \boldsymbol{0}$.*

Note that by the described rotation symmetry the particular choice of a standard position (which may vary by a rotation about **i**-axis) does not matter.

From the computational point of view, this also motivates us to define the algorithm for constructing spatial cubic PH biarcs in the following way. The C^1 Hermite data should first be transformed to the standard position, where the two-parameter family of interpolating PH cubic biarcs is computed. Then the solutions are transformed back to the original position. The whole procedure is summarized in Algorithm 1.

From now on, the parameters α and β will always denote the parameters used to construct the interpolants after the data transformation to the standard position.

Example 1. Let us consider the C^1 spatial Hermite data

$$\boldsymbol{P}_0 = (2, 2, 1)^\top, \boldsymbol{P}_2 = (1, 1, 1)^\top, \boldsymbol{t}_0 = (1, 1, 1)^\top, \boldsymbol{t}_2 = (1, 1, -2)^\top,$$

and let $\tau = 1/2$. In Fig. 1 examples of cubic PH biarcs for parameters $\alpha, \beta \in \{-\pi, -\pi/2, 0, \pi/2\}$ obtained using Algorithm 1 are shown.

Algorithm 1 C^1 Hermite interpolation by spatial PH cubic biarcs

Require: Points $\boldsymbol{P}_0$, $\boldsymbol{P}_2$ with associated tangent vectors $\boldsymbol{t}_0$, $\boldsymbol{t}_2$, parameter $\tau \in (0,1)$.
Ensure: PH cubic biarc

$$\boldsymbol{p}_\tau(t) = \begin{cases} \boldsymbol{b}(t), & t \in [0,\tau) \\ \boldsymbol{c}(t), & t \in [\tau,1] \end{cases}.$$

1: Transform data to the standard position using a transformation $\Phi : \mathbb{R}^3 \to \mathbb{R}^3$, $\Phi(\boldsymbol{x}) = R \cdot (\boldsymbol{x} - \boldsymbol{P}_0)$, with

$$R := R(\mathcal{U}) := \frac{1}{\|\mathcal{U}\|^2} \begin{pmatrix} u_0^2+u_1^2-u_2^2-u_3^2 & 2(u_1u_2-u_0u_3) & 2(u_1u_3+u_0u_2) \\ 2(u_1u_2+u_0u_3) & u_0^2-u_1^2+u_2^2-u_3^2 & 2(u_2u_3-u_0u_1) \\ 2(u_1u_3-u_0u_2) & 2(u_2u_3+u_0u_1) & u_0^2-u_1^2-u_2^2+u_3^2 \end{pmatrix},$$

$$\mathcal{U} := (u_0,u_1,u_2,u_3) = \left(\cos\frac{\phi}{2}, \sin\frac{\phi}{2}\boldsymbol{a}\right),$$

where the rotation axis $\boldsymbol{a}$ and the rotation angle ϕ are given as

$$\boldsymbol{a} = \frac{1}{\|\boldsymbol{t}_0+\boldsymbol{t}_2\|}(\boldsymbol{t}_0+\boldsymbol{t}_2)\times(1,0,0)^\top, \quad \cos\phi = \frac{1}{\|\boldsymbol{t}_0+\boldsymbol{t}_2\|}(\boldsymbol{t}_0+\boldsymbol{t}_2)\cdot(1,0,0)^\top.$$

Therefore one obtains

$$\widetilde{\boldsymbol{P}}_0 = \Phi(\boldsymbol{P}_0) = \boldsymbol{0}, \quad \widetilde{\boldsymbol{P}}_2 = \Phi(\boldsymbol{P}_2), \quad \widetilde{\boldsymbol{t}}_0 = \Phi(\boldsymbol{t}_0), \quad \widetilde{\boldsymbol{t}}_2 = \Phi(\boldsymbol{t}_2).$$

2: Compute the preimage of a PH cubic biarc

$$\mathcal{B}_0 = \mathcal{B}_0(\alpha) = \mathcal{X}(\alpha;\tau\widetilde{\boldsymbol{t}}_0), \quad \mathcal{C}_1 = \mathcal{C}_1(\beta) = \mathcal{X}(\beta;(1-\tau)\widetilde{\boldsymbol{t}}_2),$$
$$\mathcal{B}_1 = \mathcal{B}_1(\alpha,\beta) = -\frac{\tau}{2}\left(\mathcal{B}_0 + \sqrt{\frac{1-\tau}{\tau}}\mathcal{C}_1 - \mathcal{X}_p\left(\left(\mathcal{B}_0 + \sqrt{\frac{1-\tau}{\tau}}\mathcal{C}_1\right)^{2\star} - \frac{4}{\tau}(\mathcal{B}_0^{2\star} + \mathcal{C}_1^{2\star} - 3\widetilde{\boldsymbol{p}}_2)\right)\right)$$

3: Compute the control points and parameterizations of the arcs of the PH cubic biarc

$$\boldsymbol{b}_0 = \boldsymbol{P}_0,\ \boldsymbol{b}_1 = \boldsymbol{b}_0 + \frac{1}{3}\Phi^{-1}\left(\mathcal{B}_0^{2\star}\right),\ \boldsymbol{b}_2 = \boldsymbol{b}_1 + \frac{1}{3}\Phi^{-1}\left(\mathcal{B}_0\star\mathcal{B}_1\right),\ \boldsymbol{b}_3 = \boldsymbol{b}_2 + \frac{1}{3}\Phi^{-1}\left(\mathcal{B}_1^{2\star}\right),$$
$$\boldsymbol{c}_3 = \boldsymbol{P}_2,\ \boldsymbol{c}_2 = \boldsymbol{c}_3 - \frac{1}{3}\Phi^{-1}\left(\left(\sqrt{\frac{1-\tau}{\tau}}\mathcal{B}_1\right)^{2\star}\right),\ \boldsymbol{c}_1 = \boldsymbol{c}_2 - \frac{1}{3}\Phi^{-1}\left(\sqrt{\frac{1-\tau}{\tau}}\mathcal{B}_1\star\mathcal{C}_1\right),$$
$$\boldsymbol{c}_0 = \boldsymbol{c}_1 - \frac{1}{3}\Phi^{-1}\left(\mathcal{C}_1^{2\star}\right), \qquad \boldsymbol{b}(t) = \sum_{i=0}^{3}\boldsymbol{b}_i B_i^3\left(\frac{t}{\tau}\right), \quad \boldsymbol{c}(t) = \sum_{i=0}^{3}\boldsymbol{c}_i B_i^3\left(\frac{t-\tau}{1-\tau}\right).$$

Remark 1. Let us compare our construction of spatial cubic PH biarcs for C^1 Hermite data with the construction of PH quintic interpolants, which are usually used in this case. From the point of view of computational complexity, both method are equivalent because three quadratic $\star$-equations must be solved and a two-parametric system of solutions is obtained in both cases (cf. [16]).

Further, let us mention that the approximation order is one less for PH cubic biarcs than for PH quintics (see Section 4 and [16]). On the other hand, the main advantages of PH cubic biarcs over PH quintics lie in the lower degree of interpolants and in the presence of an additional free shape parameter, i.e., whereas there exists one-parameter family of PH cubic biarcs for given C^1 data with the maximal approximation order, there is a unique single PH

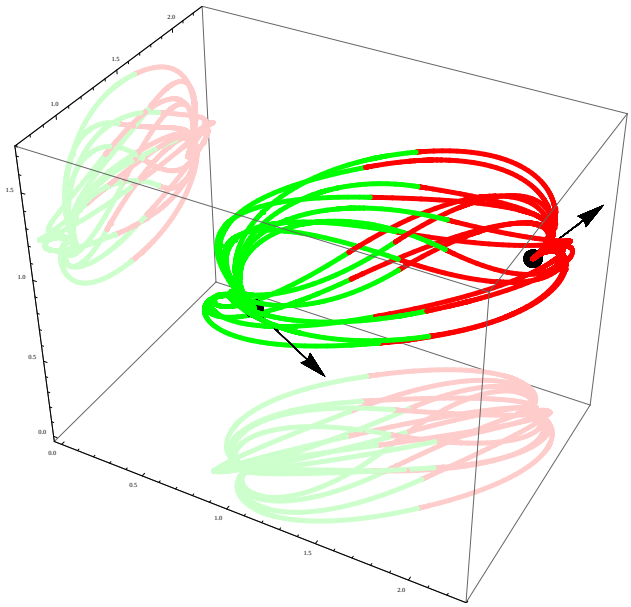

Figure 1: PH cubic biarcs obtained for input Hermite data in Example 1 for pairs of parameters (α, β), where $\alpha, \beta \in \{-\pi, -\pi/2, 0, \pi/2\}$, and $\tau = \frac{1}{2}$.

quintic interpolant with the maximal approximation order.

Finally, it is also possible to compare curvature and torsion profiles of interpolants produced by both methods, which is done for particular data in Example 2.

Example 2. Let us consider the C^1 spatial Hermite data

$$\boldsymbol{P}_0 = (0,0,0)^\top, \boldsymbol{P}_1 = (1,1,1)^\top, \boldsymbol{P}_2 = (2,2,1)^\top, \boldsymbol{P}_3 = (4,-1,-\frac{1}{2})^\top,$$
$$\boldsymbol{t}_0 = (1,-1,-1)^\top, \boldsymbol{t}_1 = (-1,2,3)^\top, \boldsymbol{t}_2 = (2,0,0)^\top, \boldsymbol{t}_3 = (-1,-1,-3)^\top.$$

Fig. 2 shows the comparison of PH quintic interpolants and PH cubic biarcs for two particular choices of the shape parameter τ. In Fig. 3 curvature and torsion profiles of these interpolating spline curves are shown. It can be seen that a particular choice of τ influences curvature and torsion profile of a resulting PH cubic spline curve.

4. Approximation order

Algorithm 1 can be used to formulate a simple method for conversion of an arbitrary regular spatial parametric curve into a C^1 spatial PH cubic spline curve. Let $\boldsymbol{f} : [0,1] \to \mathbb{R}^3$ be a regular spatial curve and let n be a number of segments. First, we sample C^1 spatial Hermite data from $\boldsymbol{f}$,

$$\boldsymbol{P}_{2i} = \boldsymbol{f}\left(\frac{i}{n}\right), \quad \boldsymbol{t}_{2i} = \boldsymbol{f}'\left(\frac{i}{n}\right), \quad i = 0,1,\ldots,n.$$

Then, we compute an interpolating PH cubic biarc $\boldsymbol{p}_\tau^i(t;\alpha,\beta)$ for each pair of consecutive sample points and associated tangent vectors $(\boldsymbol{P}_{2i}, \boldsymbol{P}_{2(i+1)}, \boldsymbol{t}_{2i}, \boldsymbol{t}_{2(i+1)})$, $i = 0,1,\ldots,n-1$, and after a linear reparameterization we obtain a C^1 spatial PH cubic spline curve ${}^n\boldsymbol{p}_\tau(t;\alpha,\beta)$. Finally, we evaluate the approximation error by measuring the Hausdorff distance

$$\mathrm{dist}_H\left(\boldsymbol{f}, {}^n\boldsymbol{p}_\tau\right) := \max\left(\max_{u\in[0,1]}\left(\min_{t\in[0,1]}||\boldsymbol{f}(t) - {}^n\boldsymbol{p}_\tau(u;\alpha,\beta)||\right), \max_{t\in[0,1]}\left(\min_{u\in[0,1]}||\boldsymbol{f}(t) - {}^n\boldsymbol{p}_\tau(u;\alpha,\beta)||\right)\right). \quad (18)$$

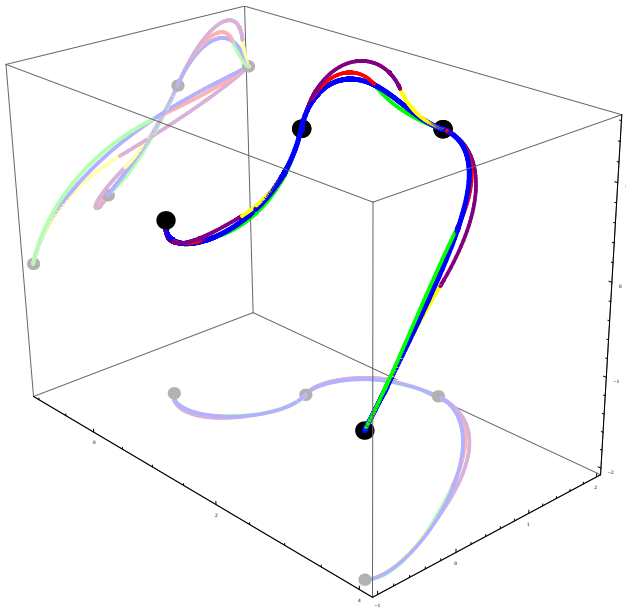

Figure 2: PH quintic interpoants (blue) and PH cubic biarcs ($\tau = 1/2$ (red, green), $\tau = 2/3$ (purple, yellow)) obtained for input Hermite data in Example 1 for $\alpha = 0, \beta = 0$.

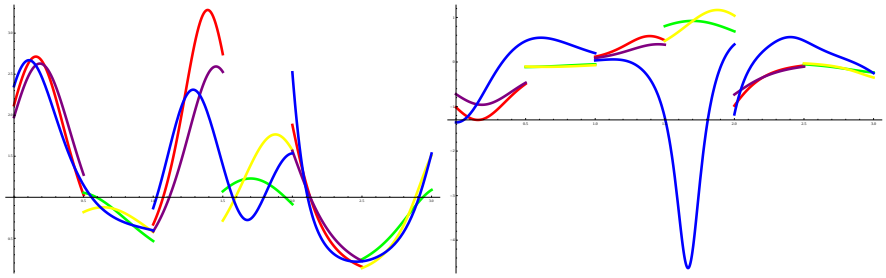

Figure 3: The comparison of curvature (left) and torsion (right) profiles for PH quintic interpoants (blue) and PH cubic biarcs ($\tau = 1/2$ (red, green), $\tau = 2/3$ (purple, yellow)) obtained for input Hermite data in Example 1 for $\alpha = 0, \beta = 0$.

If the error is not sufficiently small, we increase the number of segments and repeat the whole process.

Example 3. Let us consider a Bézier curve with control points $(2,0,0)^\top$, $(1,1,1)^\top$, $(-3,1,2)^\top$, $(0,-3,2)^\top$, $(5,0,3)^\top$ and $(-1,2,3.2)^\top$ (see Fig. 4). Table 1 summarizes the approximation error and its decay exponent (the binary logarithm of the ratio of two consecutive errors). Two particular choices of parameters $\alpha = \beta = 0$ and $\alpha = \frac{\pi}{2}$, $\beta = 0$ are considered for $\tau = \frac{1}{2}$. The decay exponent in the first case indicates that the approximation order of the curve approximation by the above mentioned procedure is 3. For parameters $\alpha = \frac{\pi}{2}$, $\beta = 0$ the approximation error decreases slower and the asymptotic approximation order is only one.

As it was shown in the previous example, not all choices of parameters α and β provide the same approximation order. As already observed for biarcs in [7], the approximation order obtained for $\alpha = \beta = 0$ is the best what we can expect. To analyse this more precisely and to identify suitable choices of parameters α and β, we will study an asymptotical behaviour of solutions $\boldsymbol{p}_\tau(t;\alpha,\beta)$. More precisely, our C^1 spatial Hermite data will be taken from an analytical curve $\boldsymbol{f} : [0,h] \to \mathbb{R}^3$ and an asymptotic analysis of solutions $\boldsymbol{p}_\tau(t;\alpha,\beta)$ will be investigated for decreasing values of h. As an error measure, we take the parametric distance introduced in [24], which is an upper bound for

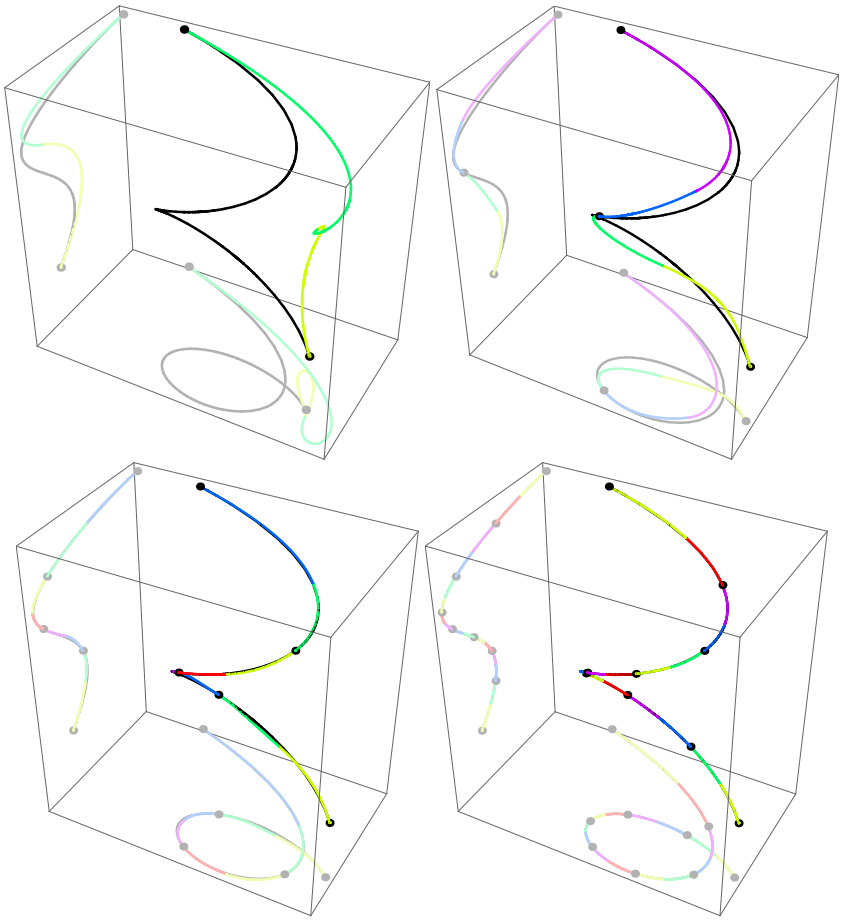

Figure 4: Bézier curve and its approximation by C^1 spatial PH cubic spline curve for n segments: $n = 1$ (top left), $n = 2$ (top right), $n = 4$ (bottom left) and $n = 8$ (bottom right).

the Hausdorff distance. The parametric distance between parametric curves $\boldsymbol{f} : [c, d] \to \mathbb{R}^d$ and $\boldsymbol{g} : [a, b] \to \mathbb{R}^d$, is defined as

$$\text{dist}_P\left(\boldsymbol{f}, \boldsymbol{g}\right) := \inf_{\psi} \max_{a \le t \le b} \| \left(\boldsymbol{f} \circ \psi\right)(t) - \boldsymbol{g}(t) \|, \tag{19}$$

where the infimum is taken among all diffeomorphisms $\psi : [a, b] \to [c, d]$, and $\|\cdot\|$ is the usual Euclidean norm. Any particular reparameterization ψ gives an upper bound on the parametric distance (19).

Theorem 2. *Let $\boldsymbol{f} : [0, h] \to \mathbb{R}^3$, $s \mapsto \boldsymbol{f}(s)$, be an analytical parametric curve parameterized by the arc-length and let $\psi : [0, 1] \to [0, h]$, $t \mapsto ht$ be the reparameterization. Further let $\boldsymbol{p}_\tau(t; \alpha, \beta) : [0, 1] \to \mathbb{R}^3$ be a spatial C^1 PH cubic biarc spline approximation with respect to an arbitrary fixed $\tau \in (0, 1)$, which satisfies*

$$\boldsymbol{p}_\tau(0; \alpha, \beta) = \boldsymbol{f}(\psi(0)) = \boldsymbol{f}(0) =: \boldsymbol{P}_0, \quad \boldsymbol{p}_\tau(1; \alpha, \beta) = \boldsymbol{f}(\psi(1)) = \boldsymbol{f}(h) =: \boldsymbol{P}_2,$$

and

$$\frac{d\boldsymbol{p}_\tau(0; \alpha, \beta)}{dt} = \frac{d(\boldsymbol{f} \circ \psi)(0)}{dt} = h\frac{d\boldsymbol{f}(0)}{ds} =: \boldsymbol{t}_0, \qquad \frac{d\boldsymbol{p}_\tau(1; \alpha, \beta)}{dt} = \frac{d(\boldsymbol{f} \circ \psi)(1)}{dt} = h\frac{d\boldsymbol{f}(h)}{ds} =: \boldsymbol{t}_2.$$

Then for $\alpha = \beta = 0$ the approximation error satisfies

$$\mathit{dist}_P\left(\boldsymbol{f}, \boldsymbol{p}_\tau\right) \le \max_{t \in [0,1]} \|(\boldsymbol{f} \circ \psi)(t) - \boldsymbol{p}_\tau(t; 0, 0)\| = \mathcal{O}\left(h^3\right).$$

Table 1: Hausdorff distance and the approximation order for Example 3.

	$\alpha=\beta=0$		$\alpha=\frac{\pi}{2},\beta=0$	
Segments (n)	$\mathrm{dist}_H\left(\boldsymbol{f},^n \boldsymbol{p}_\tau\right)$	Decay	$\mathrm{dist}_H\left(\boldsymbol{f},^n \boldsymbol{p}_\tau\right)$	Decay
2	2.71094×10^{-1}	-	4.07333×10^{-1}	-
4	1.79493×10^{-2}	3.91679	9.00869×10^{-2}	2.17682
8	3.04503×10^{-3}	2.5594	2.73028×10^{-2}	1.72227
16	4.20046×10^{-4}	2.85784	7.61397×10^{-3}	1.84233
32	6.17968×10^{-5}	2.76494	2.01659×10^{-3}	1.91673
64	7.58439×10^{-6}	3.02643	5.19698×10^{-4}	1.95617
128	9.38429×10^{-7}	3.01471	1.32751×10^{-4}	1.96895
256	1.16691×10^{-7}	3.00756	3.44051×10^{-5}	1.94803
512	1.4548×10^{-8}	3.0038	9.61148×10^{-6}	1.83979
1024	1.8161×10^{-9}	3.0019	3.24925×10^{-6}	1.56465
2048	2.26864×10^{-10}	3.00095	1.36417×10^{-6}	1.25208
4096	2.83489×10^{-11}	3.00046	6.49193×10^{-7}	1.07131

For other constant choices of α and β, the parametric distance for the particular reparameterization ψ behaves only as $\mathcal{O}(h)$.

PROOF. Without loss of generality, we may assume

$$\boldsymbol{f}(0)=\begin{pmatrix}0\\0\\0\end{pmatrix},\quad \boldsymbol{f}'(0)=\begin{pmatrix}1\\0\\0\end{pmatrix},\quad \boldsymbol{f}''(0)=\left\|\boldsymbol{f}''(0)\right\|\begin{pmatrix}0\\1\\0\end{pmatrix}. \tag{20}$$

Suppose that the curvature κ and the torsion ϱ of the curve $\boldsymbol{f}$ at $s=0$ expand as

$$\kappa(s)=\kappa_0+\kappa_1 s+\frac{\kappa_2}{2}s^2+\frac{\kappa_3}{3!}s^3+\mathcal{O}(s^4),\quad \varrho(s)=\varrho_0+\varrho_1 s+\frac{\varrho_2}{2}s^2+\frac{\varrho_3}{3!}s^3+\mathcal{O}(s^4),$$

where $\kappa_0>0$. Then (see [25]) the Frenet-Serret formulae give an expansion of the curve, simplified by the assumptions (20) to

$$\boldsymbol{f}(s)=\begin{pmatrix} s-\frac{1}{6}\kappa_0^2 s^3-\frac{1}{8}\kappa_0\kappa_1 s^4\\ \frac{1}{2}\kappa_0 s^2+\frac{1}{6}\kappa_1 s^3+\frac{1}{24}\left(-\kappa_0^3-\varrho_0^2\kappa_0+\kappa_2\right)s^4\\ \frac{1}{6}\kappa_0\varrho_0 s^3+\frac{1}{24}\left(2\kappa_1\varrho_0+\kappa_0\varrho_1\right)s^4\end{pmatrix}+\mathcal{O}\left(s^5\right). \tag{21}$$

From (21), it is straightforward to obtain expansions of the data

$$\boldsymbol{P}_0=(0,0,0)^\top,\quad \boldsymbol{P}_2=\left(h-\frac{1}{6}\kappa_0^2h^3,\frac{1}{2}\kappa_0h^2+\frac{1}{6}\kappa_1h^3,\frac{1}{6}\kappa_0\varrho_0h^3\right)^\top+\mathcal{O}\left(h^4\right),$$
$$\boldsymbol{t}_0=(h,0,0)^\top,\quad \boldsymbol{t}_2=\left(h-\frac{1}{2}\kappa_0^2h^3,\kappa_0h^2+\frac{1}{2}\kappa_1h^3,\frac{1}{2}\kappa_0\varrho_0h^3\right)^\top+\mathcal{O}\left(h^4\right).$$

Then, we follow Algorithm 1 in order to obtain the expansion of the interpolating PH cubic biarc:

Step 1. Given Hermite data can be transformed to the standard position using the quaternion multiplication

$$U(\mathbf{q})=\mathcal{U}\mathbf{q}\bar{\mathcal{U}},$$

where

$$\mathcal{U}=\left(1-\frac{1}{32}\kappa_0^2h^2,0,\frac{1}{8}\kappa_0\varrho_0h^2,-\frac{1}{4}\kappa_0h-\frac{1}{8}\kappa_1h^2\right)^\top+\mathcal{O}\left(h^3\right).$$

Then

$$\begin{aligned}
\widetilde{\boldsymbol{P}}_0 &= U(\boldsymbol{P}_0) = (0,0,0)^\top,\\
\widetilde{\boldsymbol{t}}_0 &= U(\boldsymbol{t}_0) = \left(h - \frac{1}{8}\kappa_0^2 h^3, -\frac{1}{2}\kappa_0 h^2 - \frac{1}{4}\kappa_1 h^3, -\frac{1}{4}\kappa_0\varrho_0 h^3\right)^\top + \mathcal{O}\left(h^4\right),\\
\widetilde{\boldsymbol{P}}_2 &= U(\boldsymbol{P}_2) = \left(h - \frac{1}{24}\kappa_0^2 h^3, -\frac{1}{12}\kappa_1 h^3, -\frac{1}{12}\kappa_0\varrho_0 h^3\right)^\top + \mathcal{O}\left(h^4\right),\\
\widetilde{\boldsymbol{t}}_2 &= U(\boldsymbol{t}_2) = \left(h - \frac{1}{8}\kappa_0^2 h^3, \frac{1}{2}\kappa_0 h^2 + \frac{1}{4}\kappa_1 h^3, \frac{1}{4}\kappa_0\varrho_0 h^3\right)^\top + \mathcal{O}\left(h^4\right).
\end{aligned}$$

Step 2. We now compute the expansions of preimages

$$\begin{aligned}
\mathcal{B}_0 = \Big(&-\sqrt{\tau}\sin(\alpha)\sqrt{h} + \frac{1}{32}\sqrt{\tau}\sin(\alpha)\kappa_0^2 h^{5/2}, \sqrt{\tau}\cos(\alpha)\sqrt{h} - \frac{1}{32}\left(\sqrt{\tau}\cos(\alpha)\kappa_0^2\right)h^{5/2},\\
&-\frac{1}{4}\left(\sqrt{\tau}\cos(\alpha)\kappa_0\right)h^{3/2} + \left(-\frac{1}{8}\sqrt{\tau}\cos(\alpha)\kappa_1 - \frac{1}{8}\sqrt{\tau}\sin(\alpha)\kappa_0\varrho_0\right)h^{5/2},\\
&\frac{1}{4}\sqrt{\tau}\sin(\alpha)\kappa_0 h^{3/2} + \frac{1}{8}\sqrt{\tau}\left(\sin(\alpha)\kappa_1 - \cos(\alpha)\kappa_0\varrho_0\right)h^{5/2}\Big)^\top + \mathcal{O}\left(h^{7/2}\right),\\
\mathcal{C}_1 = \Big(&-\sqrt{1-\tau}\sin(\beta)\sqrt{h} + \frac{1}{32}\sqrt{1-\tau}\sin(\beta)\kappa_0^2 h^{5/2}, \sqrt{1-\tau}\cos(\beta)\sqrt{h} - \frac{1}{32}\left(\sqrt{1-\tau}\cos(\beta)\kappa_0^2\right)h^{5/2},\\
&\frac{1}{4}\sqrt{1-\tau}\cos(\beta)\kappa_0 h^{3/2} + \frac{1}{8}\sqrt{1-\tau}\left(\cos(\beta)\kappa_1 + \sin(\beta)\kappa_0\varrho_0\right)h^{5/2},\\
&-\frac{1}{4}\left(\sqrt{1-\tau}\sin(\beta)\kappa_0\right)h^{3/2} + \frac{1}{8}\sqrt{1-\tau}\left(\cos(\beta)\kappa_0\varrho_0 - \sin(\beta)\kappa_1\right)h^{5/2}\Big)^\top + \mathcal{O}\left(h^{7/2}\right).
\end{aligned}$$

Further, we compute the expansion of $\mathcal{B}_1$, which is rather too long to include it into the paper.

Step 3. Finally, we obtain the expansions of all control points for both arcs forming an interpolating PH cubic biarc and their corresponding parameterizations, which are again too long for the inclusion into the paper (even their leading terms). Nevertheless, if we study the leading term with respect to h of the x-component of the first arc,

$$\begin{aligned}
&\Bigg(t + t^2\frac{\cos(\alpha)\sqrt{2\tau^2-2(\tau-1)\tau\cos(\alpha-\beta)-2\tau+9}+(\tau-1)\cos(\alpha-\beta)-\tau-2}{2\tau}\\
&-t^3\frac{-2\tau^2+2(\tau^2-1)\cos(\alpha-\beta)-7+((1-\tau)\cos\beta+(\tau+2)\cos\alpha)\sqrt{2\tau^2-2(\tau-1)\tau\cos(\alpha-\beta)-2\tau+9}}{6\tau^2}\Bigg)h,
\end{aligned} \tag{22}$$

the coefficients of t^2 and t^3 have to be equal to zero in order the interpolant to match the shape of $\boldsymbol{f}$. Using a computer algebra system we can solve this system of equations. It turns out that the only solution is $\alpha = \beta = 0$, independently of parameter τ. Substituting these parameters into the expansions of both arcs $\boldsymbol{b}(t)$ and $\boldsymbol{c}(t)$ of PH cubic biarc $\boldsymbol{p}_\tau(t;0,0)$ (after applying $U^\top$), we obtain

$$\begin{aligned}
\boldsymbol{b}(t) &= \left(th + \frac{\kappa_0^2}{24}\left(-2t^3 + \left(\frac{1-3\tau}{\tau}\right)t^2\right)h^3, \frac{\kappa_0}{2}t^2h^2 + \frac{\kappa_1(3\tau-1)}{12\tau}t^2h^3, \frac{\kappa_0\varrho_0(3\tau-1)}{12\tau}t^2h^3\right)^\top + \mathcal{O}\left(h^4\right),\\
\boldsymbol{c}(t) &= \Bigg(th + \frac{\kappa_0^2}{24(\tau-1)}\left(-2(\tau-1)t^3 + (4-3\tau)t^2 - 2t + \tau\right)h^3, \frac{\kappa_0}{2}t^2h^2 +\\
&\qquad \frac{\kappa_1}{12(\tau-1)}\left((3\tau-4)t^2 + 2t - \tau\right)h^3, \frac{\kappa_0\varrho_0}{12(\tau-1)}\left((3\tau-4)t^2 + 2t - \tau\right)h^3\Bigg)^\top + \mathcal{O}\left(h^4\right).
\end{aligned}$$

Therefrom we obtain the upper bound for the parametric distance

$$\max_{t\in[0,1]}\|(\boldsymbol{f}\circ\psi)(t) - \boldsymbol{p}_\tau(t;0,0)\| = \frac{\sqrt{4\kappa_0^2\varrho_0^2 + \kappa_0^4 + 4\kappa_1^2}}{24}\max\left(K_1, K_2\right)h^3 + \mathcal{O}\left(h^4\right)$$

where

$$K_1^2 := \max\left(\frac{(1-3\tau)^6}{729\tau^6}, \tau^2(1-3\tau+2\tau^2)^2\right), \quad K_2^2 := \max\left(\frac{(2-3\tau)^6}{729(\tau-1)^6}, (1-2\tau)^2(\tau-1)^2\tau^2\right).$$

Thus we have shown that the asymptotic approximation order for $\alpha = \beta = 0$ is three. Furthermore, from (22) it follows that for any other pair of constants $(\alpha, \beta) \neq (0, 0)$ the parametric distance with respect to the chosen function ψ behaves only as $\mathcal{O}(h)$. □

5. Identification of planar solutions for planar input data

Recently, planar C^1 Hermite interpolation by the so-called TC-biarcs, i.e., biarcs composed of two arcs of Tschirnhausen cubic joined with C^1 continuity, was studied in [20]. Any non-degenerate C^1 Hermite data can be interpolated by four distinct TC-biarcs which can be found by computing two complex square roots and solving one quadratic equation. Similarly to the case of C^1 planar PH quintic interpolation, these solutions can be labeled as $(++)$, $(+-)$, $(-+)$, $(--)$, where $+$, $-$ correspond to the signs of complex square roots.

Obviously, one could expect that such planar solutions will be obtained by Algorithm 1 if the input data are planar. In the following proposition, we will identify parameters α, β for which these planar solutions are obtained.

Proposition 1. *For any planar C^1 Hermite data $\boldsymbol{P}_i$, $\boldsymbol{t}_i$, $i = 0, 2$, the four PH cubic biarcs $\boldsymbol{p}_\tau(t; 0, 0)$, $\boldsymbol{p}_\tau(t; 0, -\pi)$, $\boldsymbol{p}_\tau(t; -\pi, 0)$, $\boldsymbol{p}_\tau(t; -\pi, -\pi)$, obtained by Algorithm 1, are planar and correspond to $(++)$, $(+-)$, $(-+)$, $(--)$ solutions of the planar interpolation problem with TC-biarcs, presented in [20], respectively.*

PROOF. Let us follow the idea of the proof in [16, Theorem 4]. Without loss of generality we can assume that the given C^1 Hermite data lie in the $\mathbf{ij}$-plane. Then, for any $\mathcal{A} = a_1\mathbf{i} + a_2\mathbf{j} \in \mathbb{H}$ expression (2) (for $\varphi \in \{-\pi, 0\}$) reduces to the expression for complex square root of the associated complex number, i.e., to $\pm\sqrt{a_1 + a_2\mathrm{i}} \in \mathbb{C}$, $\mathrm{i} := \sqrt{-1}$. Here we have used the identification $z_1 + \mathrm{i}z_2 \in \mathbb{C} \approx z_1\mathbf{i} + z_2\mathbf{j} \in \mathbb{H}$. With this identification at hand, operation $\star$ behaves like the standard multiplication of complex numbers. Thus, expressions for $\mathcal{B}_0$ and $\mathcal{C}_1$ for $\alpha, \beta \in \{-\pi, 0\}$ and for $\mathcal{B}_1$ (cf. Step 1 in Algorithm 1) correspond exactly to expressions for $\mathbf{w}_0$, $\mathbf{w}_2$, $\mathbf{w}_1$, respectively, in [20, Algorithm 2]. □

Example 4. Let us consider planar C^1 Hermite data

$$\boldsymbol{P}_0 = (0, 0, 0)^\top, \quad \boldsymbol{P}_2 = (1, 0, 0)^\top, \quad \mathbf{t}_0 = (2, 2, 0)^\top, \quad \mathbf{t}_2 = \left(2, \frac{2}{3}, 0\right)^\top.$$

Fig. 5 shows four PH cubic biarcs obtained by Algorithm 1 for $\alpha, \beta \in \{-\pi, 0\}$ and $\tau = \frac{1}{2}$. These solutions exactly correspond to the solutions of the planar problem (cf. Fig. 4 in [20]).

6. Computation of shape parameter τ

Suppose that we have already chosen parameters α and β (e.g. by Theorem 2). Now, it remains to determine the last free parameter τ (i.e., the parameter corresponding to the join point of the biarcs) to get a particular interpolant for given C^1 data. In this section we will discuss on how to compute the parameter τ with respect to the following characteristics: minimal arc length and minimal elastic bending energy.

The *arc length* of a parametric curve $\boldsymbol{f} : [0, 1] \to \mathbb{R}^3$ is determined as

$$L = \int_0^1 \left\|\boldsymbol{f}'(t)\right\| dt.$$

By using PH curves, the cumulative arc length is a polynomial function and can therefore be computed exactly. For a PH cubic $\boldsymbol{p}$ we have

$$L = \frac{1}{3}\left(\sigma_0 + \sigma_1 + \sigma_2\right), \qquad \|\boldsymbol{p}'(t)\| = \sigma(t) = \sum_{i=0}^{2} \sigma_i B_i^2(t).$$

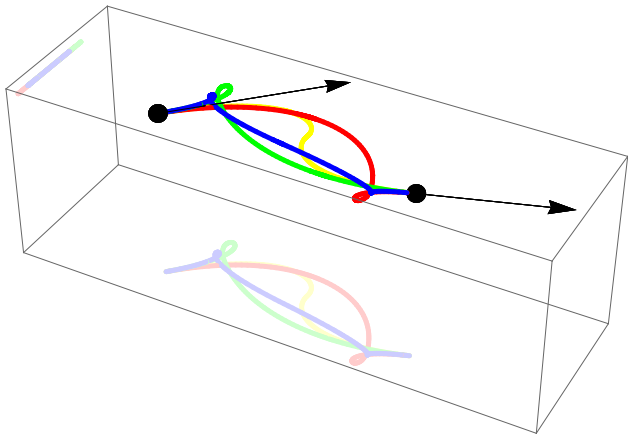

Figure 5: PH cubic biarcs obtained for planar input Hermite data in Example 4.

In the case of a PH cubic biarc the arc length L is given by the scalar part of

$$\frac{1}{3}\left(\mathcal{B}_0\bar{\mathcal{B}}_0+\frac{1}{2}\left(\mathcal{B}_0\bar{\mathcal{B}}_1+\mathcal{B}_1\bar{\mathcal{B}}_0\right)+\frac{\mathcal{B}_1\bar{\mathcal{B}}_1}{\tau}+\frac{1}{2}\sqrt{\frac{1-\tau}{\tau}}\left(\mathcal{B}_1\bar{\mathcal{C}}_1+\mathcal{C}_1\bar{\mathcal{B}}_1\right)+\mathcal{C}_1\bar{\mathcal{C}}_1\right).$$

Remark 2. Analogously to [18, Formula (64)], it can be proved that the arc length L depends only on τ and the difference $\alpha-\beta$. However, this is not of a particular importance because the only reasonable choice of the constant parameters (guaranteeing the optimal approximation order) is $(\alpha,\beta)=(0,0)$, see Theorem 2.

Example 5. Let us consider C^1 spatial Hermite data

$$\boldsymbol{P}_0=(0,0,0)^\top,\boldsymbol{P}_2=(-2,2,5)^\top,\boldsymbol{t}_0=(0,-13,20)^\top,\boldsymbol{t}_2=(4,13,-20)^\top.$$

Using Algorithm 1 and setting $\alpha=0$ and $\beta=0$ we find a family of PH cubic biarcs (depending on $\tau\in(0,1)$) interpolating given data. From this family of interpolants we choose the one which minimizes the arc length. The total arc length of the biarcs depending on $\tau\in(0,1)$ is shown in Fig. 6 (left) and the interpolant with the minimal arc length approximately equal to 11.26331, obtained for $\tau\doteq 0.83046$, is shown in Fig. 6 (right).

The next possibility for choosing a particular interpolant reflects the aspect of minimal *elastic bending energy*. Elastic bending energy ε of a curve $\mathbf{f}$ is defined as

$$\varepsilon=\int_0^1\kappa^2(t)\left\|\boldsymbol{f}'(t)\right\|dt,$$

where κ is the curvature of $\boldsymbol{f}$, defined as

$$\kappa(t)=\left\|\boldsymbol{f}'(t)\times\boldsymbol{f}''(t)\right\|/\left\|\boldsymbol{f}'\right\|^3.$$

For a PH curve $\boldsymbol{p}$ (see, e.g., [26]) we can do the following factorization

$$\left\|\boldsymbol{p}'(t)\times\boldsymbol{p}''(t)\right\|^2=\rho(t)\sigma^2(t),$$

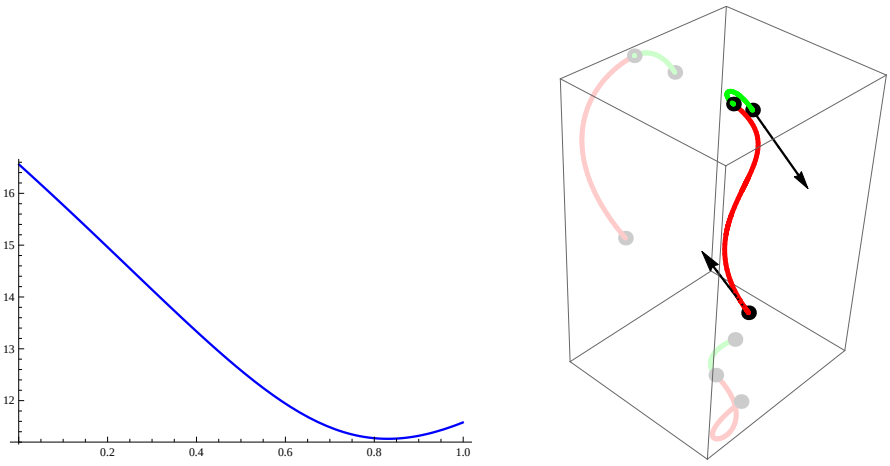

Figure 6: The total arc length of the biarcs depending on $\tau \in (0,1)$ (left) and the interpolant with the minimal arc length (right). The tangent vectors are presented six times shorter.

for some polynomial $\rho(t)$. Hence, for a PH cubic $\boldsymbol{p}$ we obtain

$$\varepsilon = \int_0^1 \frac{\|\boldsymbol{p}'(t) \times \boldsymbol{p}''(t)\|^2}{\|\boldsymbol{p}'\|^6} \|\boldsymbol{p}'\| \, dt = \int_0^1 \frac{\rho(t)\sigma^2(t)}{\|\boldsymbol{p}'\|^5} dt = \int_0^1 \frac{\rho(t)}{\sigma^3(t)} dt. \tag{23}$$

Furthermore, if $\boldsymbol{p}$ is obtained by integrating $\boldsymbol{p}' = \mathcal{B}(t)\mathbf{i}\bar{\mathcal{B}}(t)$, where $\mathcal{B}(t) = \mathcal{B}_0(1-t) + \mathcal{B}_1 t$ and $\mathcal{B}_i = (0, b_i^1, b_i^2, b_i^3)$, $i = 0, 1$, the polynomial ρ simplifies to a constant defined as

$$\rho = 4\left(\left(b_0^2 b_1^1 - b_0^1 b_1^2\right)^2 + \left(b_0^3 b_1^1 - b_0^1 b_1^3\right)^2\right),$$

which simplifies formula (23) to

$$\varepsilon = \rho \int_0^1 \sigma^{-3}(t) dt.$$

In the case of a PH cubic biarc the elastic bending energy ε is given by

$$\varepsilon = \int_0^1 \left(\frac{\rho_1}{\sigma_1^3(t)} + \frac{\rho_2}{\sigma_2^3(t)}\right) dt,$$

where

$$\rho_1 = 4\left(\left(b_0^2 b_1^1 - b_0^1 b_1^2\right)^2 + \left(b_0^3 b_1^1 - b_0^1 b_1^3\right)^2\right) \quad \text{and} \quad \rho_2 = 4\frac{1-\tau}{\tau}\left(\left(b_1^2 c_1^1 - b_1^1 c_1^2\right)^2 + \left(b_1^3 c_1^1 - b_1^1 c_1^3\right)^2\right),$$

and σ_1 and σ_2 are given by the scalar parts of

$$\mathcal{B}_0\mathcal{B}_0(1-t)^2 + (\mathcal{B}_0\mathcal{B}_1 + \mathcal{B}_1\mathcal{B}_0)(1-t)t + \mathcal{B}_1\mathcal{B}_1 t^2 \quad \text{and} \quad \frac{1-\tau}{\tau}\mathcal{B}_1\mathcal{B}_1(1-t)^2 + \sqrt{\frac{1-\tau}{\tau}}(\mathcal{B}_1\mathcal{C}_1 + \mathcal{C}_1\mathcal{B}_1)(1-t)t + \mathcal{C}_1\mathcal{C}_1 t^2,$$

respectively, and $\mathcal{B}_i = (0, b_i^1, b_i^2, b_i^3)$, $i = 0, 1$, and $\mathcal{C}_1 = (0, c_1^1, c_1^2, c_1^3)$.

Example 6. Let us consider a family of biarcs (depending on $\tau \in (0,1)$) from Example 5 and let us demonstrate a choice of the parameter τ corresponding to the minimal elastic bending energy. The energy depending on $\tau \in (0,1)$ is shown in Fig. 7 (left) and the particular biarcs with the globally minimal elastic bending energy approximately equal to 2.26853 (obtained for $\tau \doteq 0.13125$) and the locally minimal elastic bending energy approximately equal to 2.84321 (obtained for $\tau \doteq 0.72672$) are shown in Fig. 7 (right). Of course the optimal shape (with respect to minimal elastic bending energy) is provided by the global minimum only.

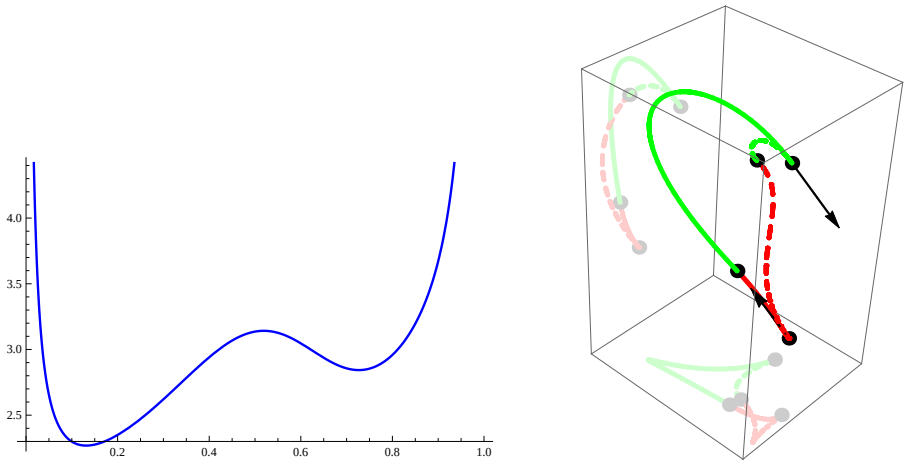

Figure 7: The elastic bending energy of the biarcs depending on $\tau \in (0,1)$ (left); and the two interpolants with the globally (solid) and locally (dashed) minimal elastic bending energy (right). The tangent vectors are presented six times shorter.

Remark 3. In Examples 5 and 6, only the parameter τ was computed in order to minimize the arc length or the elastic bending energy of the output biarc. The other two parameters α and β were both set to zero as this choice guarantees the best approximation order. However, when we give up the requirement on the best approximation order all three parameters can be considered in the the optimization process. For input data from Examples 5 and 6, the minimal arc length, approximately equal to 10.91739, is then obtained for $\alpha - \beta \doteq -1.02878$, $\tau \doteq 0.77861$, and the minimal elastic bending energy (approximately equal to 0.07504) is gained for $\alpha \doteq 1.03459$, $\beta \doteq 5.13187$, $\tau \doteq 0.71053$, see Fig 8.

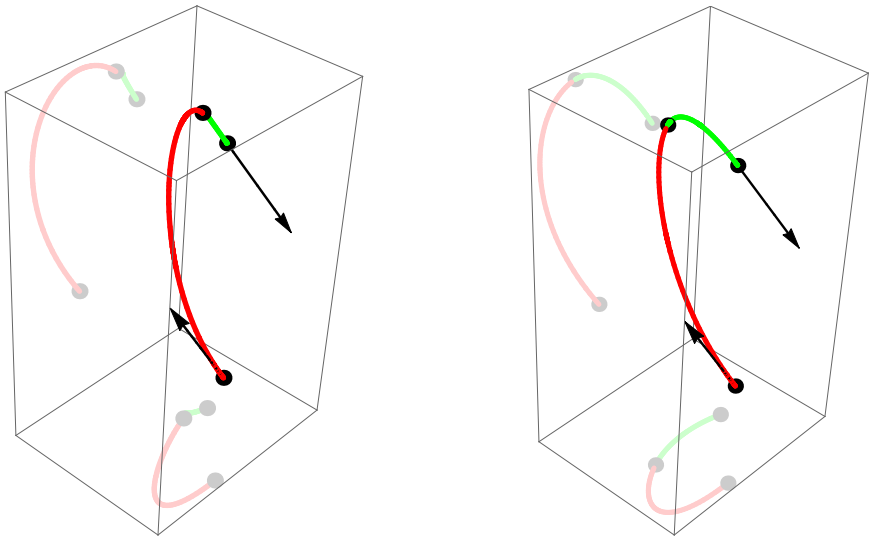

Figure 8: The biarcs with the minimal arc length (left) and the minimal elastic bending energy (right) when all parameters α, β, τ are taken into the optimization process, see Examples 5, 6 and Figures 6, 7 (right). The tangent vectors are presented six times shorter.

7. Conclusion

In this paper the problem of C^1 Hermite interpolation of spatial data by PH cubic biarcs was considered. For two given positions and two corresponding tangent vectors a PH cubic biarc was constructed. More precisely, spatial PH cubic biarc curve was constructed by joining two spatial PH cubics, each of them interpolating one position and corresponding tangent vector. Moreover, junction was done in a way that the resulting biarc became C^1 continuous. It turned out that this problem has a solution for any configuration of spatial data and the solution depends on three independent parameters. These parameters were later used to choose a particular solution with the best asymptotic approximation order (three in this case) and the minimal arc length or minimal elastic bending energy. Several numerical examples were given which confirm that the obtained biarcs are of good shape and that they can be used to approximate spatial parametric curves by PH cubic spline curves. One of the advantages of the proposed interpolation scheme is that it can be applied to any configuration of spatial data. On the other hand, the problem of Hermite C^1 interpolation by spatial PH cubics is not possible in general, and the problem of Hermite G^1 interpolation by spatial PH cubics is restricted only to particular spatial data configurations.
As a future work one could consider a generalization to C^2 Hermite interpolation by quintic biarcs. However, this problem is much more difficult which is to be expected since already a characterization of PH quintics is more complicated as it is the case of PH cubics.

Acknowledgments

All authors were supported by the Czech/Slovenian project KONTAKT MEB 091105. B. Bizzarri and M. Lávička were supported by the European Regional Development Fund (ERDF), project “NTIS - New Technologies for Information Society”, European Centre of Excellence, CZ.1.05/1.1.00/02.0090.

References

[1] R. T. Farouki, T. Sakkalis, Pythagorean hodographs, IBM J. Res. Develop. 34 (5) (1990) 736–752.
[2] D. S. Meek, D. J. Walton, Hermite interpolation with Tschirnhausen cubic spirals, Comput. Aided Geom. Design 14 (7) (1997) 619–635.
[3] R. T. Farouki, J. Peters, Smooth curve design with double-Tschirnhausen cubics, Ann. Numer. Math. 3 (1-4) (1996) 63–82, computer aided geometric design (Penang, 1994).
[4] G. Jaklič, J. Kozak, M. Krajnc, V. Vitrih, E. Žagar, On interpolation by planar cubic G^2 Pythagorean-hodograph spline curves, Math. Comp. 79 (269) (2010) 305–326.
[5] M. Byrtus, B. Bastl, G^1 Hermite interpolation by PH cubics revisited, Comput. Aided Geom. Design 27 (8) (2010) 622–630.
[6] H. P. Moon, R. T. Farouki, H. I. Choi, Construction and shape analysis of PH quintic Hermite interpolants, Comput. Aided Geom. Design 18 (2) (2001) 93–115.
[7] Z. Šír, R. Feichtinger, B. Jüttler, Approximating curves and their offsets using biarcs and Pythagorean hodograph quintics, Comput. Aided Design 38 (6) (2006) 608–618.
[8] F. Pelosi, M. L. Sampoli, R. T. Farouki, C. Manni, A control polygon scheme for design of planar C^2 PH quintic spline curves, Comput. Aided Geom. Design 24 (1) (2007) 28–52.
[9] G. Albrecht, R. T. Farouki, Construction of C^2 Pythagorean-hodograph interpolating splines by the homotopy method, Adv. Comput. Math. 5 (4) (1996) 417–442.
[10] H. I. Choi, R. T. Farouki, S.-H. Kwon, H. P. Moon, Topological criterion for selection of quintic Pythagorean-hodograph Hermite interpolants, Comput. Aided Geom. Design 25 (6) (2008) 411–433.
[11] R. T. Farouki, Pythagorean-hodograph curves: algebra and geometry inseparable, Vol. 1 of Geometry and Computing, Springer, Berlin, 2008.
[12] B. Jüttler, C. Mäurer, Cubic Pythagorean-hodograph spline curves and applications to sweep surface modeling, Comput. Aided Geom. Design 31 (1999) 73–83.
[13] F. Pelosi, R. T. Farouki, C. Manni, A. Sestini, Geometric Hermite interpolation by spatial Pythagorean-hodograph cubics, Adv. Comput. Math. 22 (4) (2005) 325–352.
[14] S.-H. Kwon, Solvability of G^1 Hermite interpolation by spatial Pythagorean-hodograph cubics and its selection scheme, Comput. Aided Geom. Design 27 (2) (2010) 138–149.
[15] G. Jaklič, J. Kozak, M. Krajnc, V. Vitrih, E. Žagar, An approach to geometric interpolation by Pythagorean-hodograph curves, Adv. Comput. Math. 37 (1) (2012) 123–150.
[16] Z. Šír, B. Jüttler, Spatial Pythagorean Hodograph Quintics and the Approximation of Pipe Surfaces, Lecture Notes in Computer Science 3604 (2005) 364–380.
[17] Z. Šír, B. Jüttler, C^2 Hermite interpolation by Pythagorean hodograph space curves, Math. Comp. 76 (259) (2007) 1373–1391 (electronic).
[18] R. T. Farouki, C. Giannelli, C. Manni, A. Sestini, Identification of spatial PH quintic Hermite interpolants with near-optimal shape measures, Computer Aided Geometric Design 25 (4-5) (2008) 274–297.
[19] R. T. Farouki, C. Manni, A. Sestini, Spatial C^2 PH quintic splines, Curve and Surface Design: Saint Malo 2002 (T. Lyche, M.-L. Mazure, and L. L. Schumaker, eds.), Nashboro Press, (2003) 147–156.

[20] B. Bastl, K. Slabá, M. Byrtus, Planar C^1 Hermite interpolation with uniform and non-uniform TC-biarcs, To appear in Comput. Aided Geom. Design.
[21] R. T. Farouki, The conformal map $z \to z^2$ of the hodograph plane, Comput. Aided Geom. Design 11 (4) (1994) 363–390.
[22] R. T. Farouki, M. al Kandari, T. Sakkalis, Hermite interpolation by rotation-invariant spatial Pythagorean-hodograph curves, Adv. Comput. Math. 17 (4) (2002) 369–383.
[23] G. Farin, Curves and surfaces for computer-aided geometric design, 4th Edition, Computer Science and Scientific Computing, Academic Press Inc., San Diego, CA, 1997.
[24] T. Lyche, K. Mørken, A metric for parametric approximation, in: Curves and surfaces in geometric design (Chamonix-Mont-Blanc, 1993), A K Peters, Wellesley, MA, 1994, pp. 311–318.
[25] E. Kreyszig, Differential geometry, Dover Publications Inc., New York, 1991, reprint of the 1963 edition.
[26] R. T. Farouki, Exact rotation-minimizing frames for spatial pythagorean-hodograph curves, Graphical Models 64 (2003) 382–395.